Anal. Chem. **2009,** *81,* 6972–6980

Derivatization of Optically Transparent Materials with Diazonium Reagents for Spectroscopy of Buried Interfaces

Amr M. Mahmoud,[†] Adam Johan Bergren,*[,‡] and Richard L. McCreery[†,‡]

University of Alberta, Edmonton, Alberta, Canada T6G 2G2, and National Institute for Nanotechnology, Edmonton, Alberta, Canada T6G 2M9

This paper presents a method to derivatize a wide variety of substrate materials that are frequently used in spectroscopic characterizations with molecular layers through the reduction of aromatic diazonium reagents. The method relies on an ultrathin (5 nm) layer of a reactive metal (e.g., Ti or Al) deposited as a primer that subsequently mediates the reduction of aromatic diazonium reagents from acetonitrile solution. Following surface modification, the Ti can be oxidized to provide a passivated support surface. Raman, Infrared, UV−vis and X-ray photoelectron spectroscopic techniques are used to characterize the molecular layers on the metal primer surface. When a Ti primer layer is derivatized via diazonium reduction, the molecule is shown to be present on the ultrathin Ti layer on Au, Al, quartz, Si/SiO_x, glass, and polyethylene surfaces. For molecules bound to a Ti primer, the molecular layer was found to be stable to sonication in acetone or acetonitrile, a 1 h exposure to boiling water, and a 30 min exposure to 0.1 M acid or base. The approach also permits spectroscopic characterization of buried thin-film molecular layers on optically transparent substrates after deposition of thick top metal contacts.

The derivatization of a wide variety of surfaces with organic compounds that possess desirable chemical or physical properties is an important technological target. Furthermore, the characterization of molecular layers on the surface of these substrates is an important consideration for many applications. This is especially important in cases where the molecular layers are incorporated into a more complex structure with a targeted function. For example, in molecular electronics, stratified layers of conductors and molecules are utilized to build devices useful for studying charge transport mechanisms or novel electronic phenomena as a function of molecular structure.[1−6] In such investigations, it is critical to establish the influence of molecular structure on the performance of the device. However, it can be difficult to probe molecular species buried in working electronic devices since the contacts and/or substrates must be transparent in the frequency range under study.[3,7−9] A general pathway to covalently bind a molecular layer to a wide range of surfaces that can be characterized using various optical spectroscopic techniques would therefore be beneficial.

The manipulation of interfaces is important in numerous areas of science and engineering. For example, advances in the design and performance of sensors,[10,11] energy conversion devices,[12] catalysts,[13] and molecular electronics[3,14−16] all rely, in part, on well-controlled surface modification. To this end, aromatic diazonium salts have been used to modify substrate surfaces having a wide range of conductivity,[17,18] including metals,[18−26] carbon,[14,18,27−31]

* To whom correspondence should be addressed. E-mail: adam.bergren@nrc.ca. Phone: (780)641-1762. Fax: (780)641-1601.
† University of Alberta.
‡ National Institute for Nanotechnology.

(1) Akkerman, H. B.; De Boer, B. *J. Phys.: Condens. Matter* **2008**, *20*, 013001.
(2) McCreery, R. *Chem. Mater.* **2004**, *16*, 4477–4496.
(3) McCreery, R. L. *Anal. Chem.* **2006**, *78*, 3490–3497.
(4) de Boer, B.; Frank, M. M.; Chabal, Y. J.; Jiang, W. R.; Garfunkel, E.; Bao, Z. *Langmuir* **2004**, *20*, 1539–1542.
(5) Wang, W.; Lee, T.; Kamdar, M.; Reed, M. A.; Stewart, M. P.; Hwang, J. J.; Tour, J. M. *Mol. Electron. III* **2003**, *1006*, 36–47.
(6) Selzer, Y.; Allara, D. *Annu. Rev. Phys. Chem.* **2006**, *57*, 593–623.
(7) Bonifas, A. P.; McCreery, R. L. *Chem. Mater.* **2008**, *20*, 3849–3856.
(8) Hipps, K. W.; Dowdy, J.; Hoagland, J. J. *Langmuir* **1991**, *7*, 5–7.
(9) Nowak, A. M.; McCreery, R. L. *J. Am. Chem. Soc.* **2004**, *126*, 16621–16631.
(10) Bergren, A. J.; Porter, M. D. *J. Electroanal. Chem.* **2007**, *599*, 12–22.
(11) Edwards, G. A.; Bergren, A. J.; Porter, M. D. *Handbook of Electrochemistry*, 1st ed.; Zoski, C. G., Ed.; Elsevier: New York, 2007, pp 295−327.
(12) Rider, D. A.; Harris, K. D.; Wang, D.; Bruce, J.; Fleischauer, M. D.; Tucker, R. T.; Brett, M. J.; Buriak, J. M. *Appl. Mater. Interfaces* **2009**, *1*, 279–288.
(13) Xu, Z. Q.; Qi, Z. G.; Kaufman, A. *Electrochem. Solid State Lett.* **2003**, *6*, A171−A173.
(14) Bergren, A. J.; Harris, K. D.; Deng, F. J.; McCreery, R. L. *J. Phys.: Condens. Matter* **2008**, *20*, 374117–374127.
(15) Kalakodimi, R. P.; Nowak, A. M.; McCreery, R. L. *Chem. Mater.* **2005**, *17*, 4939–4948.
(16) Anariba, F.; Steach, J. K.; McCreery, R. L. *J. Phys. Chem. B* **2005**, *109*, 11163–11172.
(17) Pinson, J.; Podvorica, F. *Chem. Soc. Rev.* **2005**, *34*, 429–439.
(18) Adenier, A.; Cabet-Deliry, E.; Chausse, A.; Griveau, S.; Mercier, F.; Pinson, J.; Vautrin-Ul, C. *Chem. Mater.* **2005**, *17*, 491–501.
(19) Mirkhalaf, F.; Paprotny, J.; Schiffrin, D. J. *J. Am. Chem. Soc.* **2006**, *128*, 7400–7401.
(20) Ricci, A.; Bonazzola, C.; Calvo, E. J. *Phys. Chem. Chem. Phys.* **2006**, *8*, 4297–4299.
(21) Chamoulaud, G.; Belanger, D. *J. Phys. Chem. C* **2007**, *111*, 7501–7507.
(22) Liu, G. Z.; Bocking, T.; Gooding, J. J. *J. Electroanal. Chem.* **2007**, *600*, 335–344.
(23) Pan, Q. M.; Wang, M.; Chen, W. T. *Chem. Lett.* **2007**, *36*, 1312–1313.
(24) Adenier, A.; Barre, N.; Cabet-Deliry, E.; Chausse, A.; Griveau, S.; Mercier, F.; Pinson, J.; Vautrin-Ul, C. *Surf. Sci.* **2006**, *600*, 4801–4812.
(25) Ghilane, J.; Delamar, M.; Guilloux-Viry, M.; Lagrost, C.; Mangeney, C.; Hapiot, P. *Langmuir* **2005**, *21*, 6422–6429.
(26) Hurley, B. L.; McCreery, R. L. *J. Electrochem. Soc.* **2004**, *151*, B252−B259.
(27) Allongue, P.; Delamar, M.; Desbat, B.; Fagebaume, O.; Hitmi, R.; Pinson, J.; Saveant, J. M. *J. Am. Chem. Soc.* **1997**, *119*, 201–207.
(28) Anariba, F.; DuVall, S. H.; McCreery, R. L. *Anal. Chem.* **2003**, *75*, 3837–3844.
(29) Baranton, S.; Belanger, D. *J. Phys. Chem. B* **2005**, *109*, 24401–24410.

10.1021/ac901052v CCC: $40.75
Published on Web 07/16/2009

carbon nanotubes,[32] and semiconductors.[33,34] Diazonium-mediated surface modification relies on the generation of a phenyl radical species through reduction of the diazonium group followed by elimination of N_2. The radical species interacts with a surface site, often resulting in a covalent bond, the details of which depend on the surface material.[18] In particular, when the surface in question has free electrons and if electron transfer is favorable thermodynamically, a spontaneous reduction of the diazonium salt can take place, resulting in a self-sustaining surface modification reaction.[35,36] The resulting molecular layers are generally robust, and the modified surfaces can be applied in many different studies. However, it should be noted that the aggressive nature of the radical-mediated bonding pathway readily leads to multilayer films. The thickness of these films can be controlled by adjusting the appropriate conditions (e.g., diazonium ion concentration and immersion time) and verifying thickness with atomic force microscopy.[28]

To characterize buried molecular layers as in electronic devices, several methods have been reported. Raman spectra have been obtained through thin semi-transparent top contacts.[9,15,37,38] Infrared reflection spectroscopy has been carried out through partially IR transparent Si substrates that also act as the support for the molecular layer.[39,40] In this case, thick, reflective top contacts are applied on top of the molecules to provide a highly reflective surface.[39,40] Ultraviolet−visible (UV−vis) spectroscopy has been reported for characterization of molecular layers through multiple thin layers of a completed molecular electronic device.[7] Other reported optical probes include attenuated total internal reflection (ATR) FTIR spectroscopy,[41,42] multiple transmission-reflection infrared (MTR),[43] and infrared reflectance spectroscopy.[44,45] Finally, inelastic electron tunneling spectroscopy (IETS) also provides information about molecular structure and geometry during the course of charge transfer measurements.[46−48]

In this paper, we describe the use of reactive metal primers to modify quartz, Si, glass, and other surfaces so that Raman, IRRAS, *p*-polarized backside IRRAS, and UV−vis spectroscopic measurements can be accommodated in molecular junctions and related structures. Both Ti and Al are known to form strong metal−oxygen and metal−carbon bonds with a variety of materials, and are often used as "adhesion layers." The thin metal layer also provides a suitable reducing potential at the substrate surface that drives the reduction of diazonium ions, generating radicals that can bind to the surface, leading to the formation of a molecular organic layer. After deposition of top contacts, an analysis of Raman and IR vibrational spectra can be used to test molecular integrity during these often harsh fabrication procedures. The nature of the bond formed between the metal primer and organic layer is investigated using X-ray photoelectron spectroscopy, suggesting the presence of an M−O−C covalent bond. In addition, the stability of the molecular layer on the surface was studied by subjecting primer-derived molecular layers to heating and immersion in organic solvents and aqueous acid and base. Finally, the variables affecting the characteristics of the molecular layer including immersion time, primer metal thickness, and diazonium salt concentration were also investigated.

EXPERIMENTAL SECTION

Acetonitrile, acetone, and isopropanol (HPLC grade, Fischer Scientific) were used as received. Water was purified by a Millipore system (18 MΩ, 3 ppb TOC). 4-Nitroazobenzene 4′-diazonium tetrafluoroborate salt (NAB DS) was prepared as described in detail elsewhere.[37] For Raman and UV−vis spectroscopy, 25 × 25 × 0.22 mm^3 quartz microscope coverslips (Technical Glass Products, Inc.) were used as an optically transparent support. For infrared experiments, highly infrared transparent Si was used (double-side-polished highly n-doped Si (111) from Cemat Silicon S. A.) after dicing into 18 × 15 mm^2 chips. In addition, glass (22 × 22 × 0.14 mm^3 glass cover slides from Fischer scientific) and high density polyethylene (HDPE) from Nalgene plastic bottles cut into 20 × 20 mm^2 pieces were used in other experiments. Quartz (Q), glass (G), and Si substrates were cleaned by sonication in acetone, isopropanol, and then ultrapure water for 10 min each, and HDPE substrates were cleaned by sonication in ultrapure water only; all substrates were dried after cleaning in a stream of N_2. Substrates were transferred to an electron-beam evaporator (Kurt J. Lesker PVD75), and the chamber evacuated overnight to a pressure of 2.2×10^{-7} Torr before beginning deposition. Metals (Ti, Al, and Cr) were deposited at 0.3 Å/s, as determined from a quartz crystal microbalance near the sample. Metal thicknesses are indicated in nanometers in sample designations; for example, Q/Ti(5) indicates 5 nm of Ti deposited on quartz.

Chemical derivatization of the primed surfaces was performed by the spontaneous reduction of diazonium salts in acetonitrile solution. Immediately after removing primed substrates from the evaporation chamber, they were immersed in a freshly prepared solution of the diazonium salt (1 mM) in acetonitrile for 30 min,

(30) Delamar, M.; Hitmi, R.; Pinson, J.; Saveant, J. M. *J. Am. Chem. Soc.* **1992**, *114*, 5883–5884.
(31) McCreery, R. L. *Chem. Rev.* **2008**, *108*, 2646–2687.
(32) Abiman, P.; Wildgoose, G. G.; Compton, R. G. *Int. J. Electrochem. Sci.* **2008**, *3*, 104–117.
(33) Stewart, M. P.; Maya, F.; Kosynkin, D. V.; Dirk, S. M.; Stapleton, J. J.; McGuiness, C. L.; Allara, D. L.; Tour, J. M. *J. Am. Chem. Soc.* **2004**, *126*, 370–378.
(34) Scott, A.; Janes, D. B.; Risko, C.; Ratner, M. A. *Appl. Phys. Lett.* **2007**, *91*, 033508.
(35) Combellas, C.; Delamar, M.; Kanoufi, F.; Pinson, J.; Podvorica, F. I. *Chem. Mater.* **2005**, *17*, 3968–3975.
(36) Garrett, D. J.; Lehr, J.; Miskelly, G. M.; Downard, A. J. *J. Am. Chem. Soc.* **2007**, *129*, 15456–15457.
(37) Nowak, A. M.; McCreery, R. L. *Anal. Chem.* **2004**, *76*, 1089–1097.
(38) Jaiswal, A.; Tavakoli, K. G.; Zou, S. Z. *Anal. Chem.* **2006**, *78*, 120–124.
(39) Richter, C. A.; Hacker, C. A.; Richter, L. J.; Kirillov, O. A.; Suehle, J. S.; Vogel, E. M. *Solid State Electron.* **2006**, *50*, 1088–1096.
(40) Scott, A.; Hacker, C. A.; Janes, D. B. *J. Phys. Chem. C* **2008**, *112*, 14021–14026.
(41) Anariba, F.; Viswanathan, U.; Bocian, D. F.; McCreery, R. L. *Anal. Chem.* **2006**, *78*, 3104–3112.
(42) Jun, Y. S.; Zhu, X. Y. *J. Am. Chem. Soc.* **2004**, *126*, 13224–13225.
(43) Liu, H. B.; Venkataraman, N. V.; Bauert, T. E.; Textor, M.; Xiao, S. J. *J. Phys. Chem. A* **2008**, *112*, 12372–12377.
(44) Fisher, G. L.; Walker, A. V.; Hooper, A. E.; Tighe, T. B.; Bahnck, K. B.; Skriba, H. T.; Reinard, M. D.; Haynie, B. C.; Opila, R. L.; Winograd, N.; Allara, D. L. *J. Am. Chem. Soc.* **2002**, *124*, 5528–5541.
(45) Walker, A. V.; Tighe, T. B.; Cabarcos, O. M.; Reinard, M. D.; Haynie, B. C.; Uppili, S.; Winograd, N.; Allara, D. L. *J. Am. Chem. Soc.* **2004**, *126*, 3954–3963.
(46) James, D. K.; Tour, J. M. *Anal. Chim. Acta* **2006**, *568*, 2–19.
(47) Troisi, A.; Ratner, M. A. *J. Chem. Phys.* **2006**, *125*, 214709.
(48) Yu, L. H.; Zangmeister, C. D.; Kushmerick, J. G. *Phys. Rev. Lett.* **2007**, *98*, 206803.

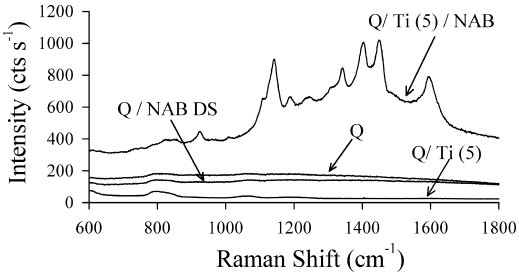

Figure 1. Raman spectra of four samples: unprimed quartz (Q) and Ti-primed quartz (Q/Ti(5)) are shown, as are both types of samples after a 30 min immersion in a 1 mM solution of NAB diazonium salt (Q/NAB DS and Q/Ti(5)/NAB). Laser and collection optics located on modified side of quartz plate, i.e., "frontside" illumination (see Scheme 1B for an example, noting that the gold is absent).

except for the modification of HDPE, which was done using aqueous 0.1 M H_2SO_4 as the solvent. Following immersion, the substrate was rinsed with neat acetonitrile (or 0.1 M H_2SO_4) and then dried in a stream of N_2. Reflective metal overlayers of Au or Ag were electron-beam deposited at 3 Å s^{-1} at a pressure of 2.6×10^{-6} Torr onto Q/primer/NAB or Si/primer/NAB substrates for "backside" Raman and IR, respectively. For XPS experiments, thermally oxidized Si samples primed with Ti were removed from the evaporation chamber and placed into a low vacuum transport chamber before being transferred to the XPS analysis chamber to minimize atmospheric exposure.

Raman spectra were collected through the transparent Q/primer substrate using a custom built spectrometer equipped with an argon ion laser (514.5 nm), a 50 mm f/1.8 Nikon camera collection lens, a 2000 groove/mm holographic reflection grating, and a back scattering geometry that employs an Andor back-thinned charge-coupled device (CCD) detector cooled to −80 °C.[49] The incident power was ~19 mW, and the signal was integrated for 30 s, unless stated otherwise. Infrared spectra were collected using a Bruker optics VERTEX 70 FT-IR spectrometer fitted with a Harrick Seagull reflection accessory and an MCT detector. Each spectrum represents the average of 512 scans and was collected using an incidence angle of 80°, *p*-polarized light, a 1 mm optical aperture, 4 cm^{-1} resolution, Blackman-Harris 3-term apodization, and a zero-filling factor of 2. Data collection was initiated after a 20 min purge with dry N_2. UV−vis spectra were recorded using a Perkin-Elmer Lambda 900 spectrometer.

RESULTS AND DISCUSSION

Titanium is a highly reactive metal that is easily oxidized in ambient conditions.[50] This reactivity can be utilized to initiate the reduction of a diazonium salt in solution, which, in turn, forms free aryl radicals that bind to the Ti surface, resulting in a chemisorbed molecular layer. Figure 1 shows Raman spectra of quartz (Q) and Q/Ti (5 nm), before and after immersion in a solution of 1 mM NAB diazonium ion in acetonitrile for 30 min. Analysis of Figure 1 shows the ultrathin Ti layer does not contribute significantly to Raman scattering since both Q and Q/Ti(5) have very similar spectra. The only features in these spectra are those expected for bare quartz, and include a longitudinal optical (LO) mode at ~807 cm^{-1} and a transverse optical (TO) mode at ~795 cm^{-1} which appear as a broad unresolved peak, and a TO mode at 1073 cm^{-1}.[51] Moreover, the absence of the molecular vibrational spectrum for NAB after immersion of Q in NAB DS shows that without the reactive metal primer, NAB is not present in a detectable quantity at this surface using Raman spectroscopy, which was also verified by XPS (data not shown). On the other hand, the NAB spectrum appears quite strong when the Q substrate is primed with a 5 nm layer of Ti (the characteristic Raman frequencies and peaks assignment for NAB on Ti surface are given in Table 1[37,41]). Furthermore, attempts to modify Q without a Ti primer layer but with a solution of reducing agent and a diazonium ion, as reported for Au and carbon nanotubes,[19,52] did not result in an observable NAB Raman spectrum on the treated quartz sample. However, to use the reactivity of Ti metal as a surface primer, it is critical that primer exposure to air is minimized. For example, after exposing a Q substrate primed with Ti metal to ambient atmospheric conditions for 3 days prior to surface modification by NAB DS, the intensity of the Raman signal for NAB was reduced by ~92% relative to that observed in Figure 1 (see Supporting Information, Figure S-1), which is attributed to the oxidation of Ti metal by atmospheric oxygen, leaving a less reactive surface for diazonium reduction. Additional characterization of the chemisorbed NAB layer is described below, but first the generality of the approach to a variety of surfaces was examined.

Table 1. Characteristic Raman Frequencies and Corresponding Assignments for NAB Molecules on Ti and Al

NAB in CCl_4	Ti/NAB	Al/NAB	assignment
933	927	922	CH bend
1112			Ph−NO_2 stretch
1147	1139	1141	Ph−N=N stretch
1183	1191	1191	CH bend
1347	1344	1341	NO_2 stretch
1412	1406	1401	N=N stretch
1449	1451	1448	N=N stretch
1594	1598	1596	C=C ring stretch

The Ti primer provides a platform for the spontaneous modification of various surfaces including quartz and Si (see below). Since Ti is known to adhere to numerous materials possessing a wide range of conductivity,[50,53,54] several different substrates were tested: Au, Al foil, SiO_x, glass, and high density polyethylene (HDPE) surfaces. Raman spectroscopy confirmed bonding of NAB to Ti primer layers on Au, Al foil, SiO_x on Si, and glass (see Supporting Information, Figures S-2 and S-3). Raman spectroscopy was not suitable for monitoring bonding to HDPE because of a large substrate Raman signal, but XPS of

(49) Ramsey, J.; Ranganathan, S.; McCreery, R. L.; Zhao, J. *Appl. Spectrosc.* **2001**, *55*, 767–773.
(50) Vogt, K. W.; Kohl, P. A.; Carter, W. B.; Bell, R. A.; Bottomley, L. A. *Surf. Sci.* **1994**, *301*, 203–213.
(51) Scott, J. F.; Porto, S. P. S. *Phys. Rev.* **1967**, *161*, 903–910.
(52) Heald, C. G. R.; Wildgoose, G. G.; Jiang, L.; Jones, T. G. J.; Compton, R. G. *ChemPhysChem* **2004**, *5*, 1794–1799.
(53) Brama, Y. L.; Sun, Y.; Dangeti, S. R. K.; Mujahid, M. *Surf. Coat. Technol.* **2005**, *195*, 189–197.
(54) Péter, M.; Furthner, F.; Deen, J.; de Laat, W. J. M.; Meinders, E. R. *Thin Solid Films* **2009**, *517*, 3081–3086.

Scheme 1. Schematic Diagram of Geometries Employed in Obtaining Raman Spectra[a]

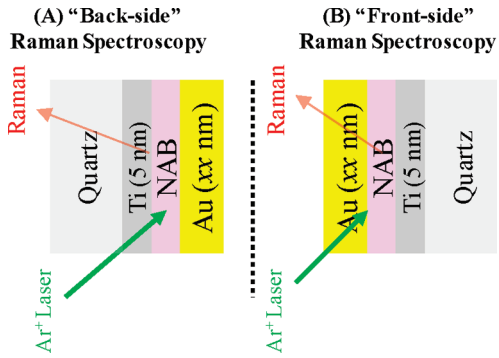

[a] (A) "Back-side" geometry, where the incident light passes through the substrate support (Quartz) before exciting the molecule. (B) "Front-side" geometry where light must pass through a metallic top layer.

HDPE following deposition of a 5 nm Ti primer layer and exposure to NAB DS solution in 0.1 M H_2SO_4 showed characteristic N(1s) peaks in both low- and high-resolution XPS spectra (see Supporting Information, Figure S-4).

In addition to Ti, Al and Cr are also widely used as adhesion layers, and bulk Al alloy surfaces have been modified electrochemically with molecular layers through diazonium chemistry.[26] Using a 5 nm layer of metallic Al as a primer to modify a quartz surface spontaneously with NAB resulted in a Raman spectrum comparable to that observed when using Ti as the primer metal. However, the intensity when using Al was ~85% that observed when using Ti (see Supporting Information, Figure S-5). On the other hand, the NAB spectrum on a similarly prepared Cr film on quartz was below the Raman detection limit (see Supporting Information, Figure S-6).

Quartz has a very low infrared transparency; however, silicon can be highly IR-transparent, depending on the details of doping.[55] Recently, a "backside" infrared reflection technique was developed to characterize aromatic molecular layers adsorbed directly on Si.[40] The method relies on the deposition of a metallic overlayer on top of the molecules to provide a reflective surface, and the spectrum is then acquired through the IR-transparent substrate. Instead of using this method for substrates in which the derivatization is carried out directly on Si, we have used metal-primed IR-transparent Si substrates. A significant portion of the infrared light incident from air onto the backside of the Si substrate passes through the Si, Ti, and molecule phases, and is reflected from the surface of the thick metal overlayer, enabling *p*-polarized backside infrared reflection absorption spectra (*p*-b IRRAS) to be obtained.

Figure 2 shows IRRAS spectra for several samples in two different geometries (as illustrated in Scheme 2) and illustrates the utility of an ultrathin metal primer in mediating the modification of Si with an organic layer. Figure 2A shows an IRRAS spectrum of NAB in the "backside" geometry, while Figure 2B shows conventional IRRAS spectra of Si/SiO_x/Cr(5)/Au(100)/Ti(5) and Si/SiO_x/Cr(5)/Au(100)/Ti(5)/NAB obtained in a conventional geometry (i.e., "frontside" spectra). These data

(55) Hilbrich, S.; Theiss, W.; ArensFischer, R.; Gluck, O.; Berger, M. G. *Thin Solid Films* **1996**, *276*, 231–234.

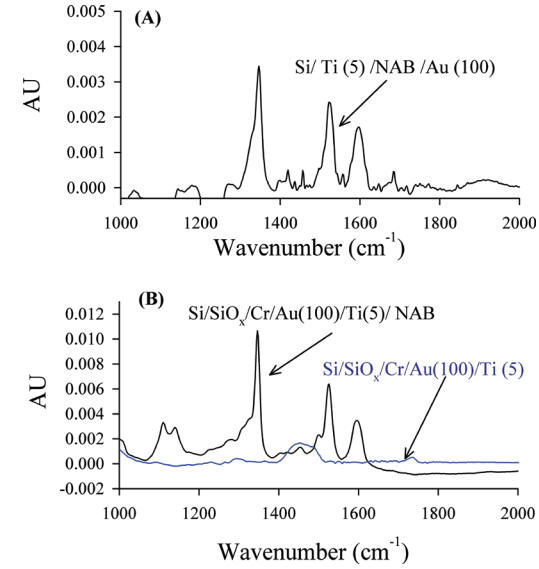

Figure 2. (A) Backside IRRAS for Si/Ti(5)/NAB/Au(100), showing the molecular signature for NAB is clearly observed. (see Scheme 2A) (B) Corresponding frontside IRRAS spectra for Au/Ti(5) (blue curve) and Au/Ti(5)/NAB (black curve), showing that the Ti primer does not have significant IR bands in this wavelength range and that the metal primer can be used to modify a gold surface. (see Scheme 2B.)

Scheme 2. Diagram of Experimental Set-up Used to Obtain IRRAS Spectra[a]

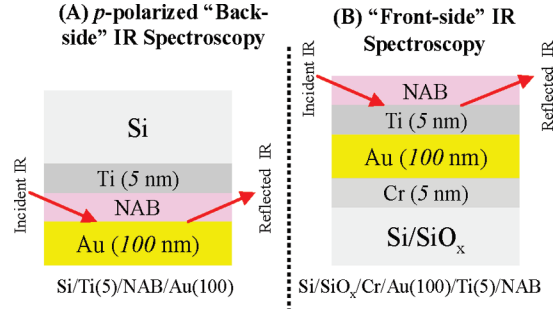

[a] (A) In the "back-side" method, light passes through IR-transparent Si, which is used at the substrate support, and is reflected from an optically dense layer of metal deposited directly onto the molecular layer. (B) In the "front-side" or conventional geometry, light must pass through any top contact materials to obtain a spectrum (no top layer is shown in the figure).

Table 2. IR Frequencies and Peak Assignments for NAB

Ti/NAB	assignment
1107	C−H/ NO_2
1136	Ph−N=N stretch
1346	NO_2
1524	NO_2 + C=C ring
1591	NO_2 + C=C ring

illustrate two important points. First, the molecular layer survives the "direct" e-beam deposition of 100 nm of Au on the Si/Ti/NAB surface as shown in Figure 2A. Second, ultrathin Ti metal can be used to prime Si surfaces to derivatize the substrate with an organic layer, and the Ti does not significantly interfere with the IR spectral signature of the molecule. The characteristic vibrational spectrum for NAB appeared only when the Ti primer was present, indicating that the metal primer is

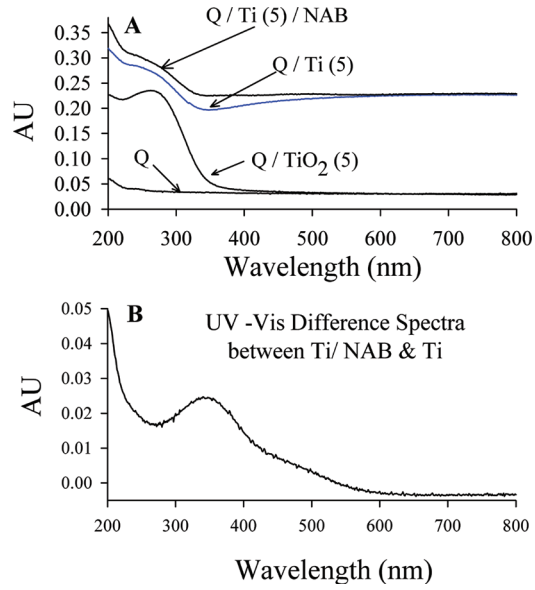

Figure 3. (A) Transmission UV−vis spectra referenced to air for several samples, as indicated. (see Scheme 3) (B) Difference spectrum plotted as the absorbance for Q/Ti(5)/NAB after subtracting the absorbance for Q/Ti(5), showing the absorbance band for NAB with a maximum at 340 nm.

Scheme 3. In UV-vis, Light Passes through the Transparent Substrate and the Transmitted Light is Detected

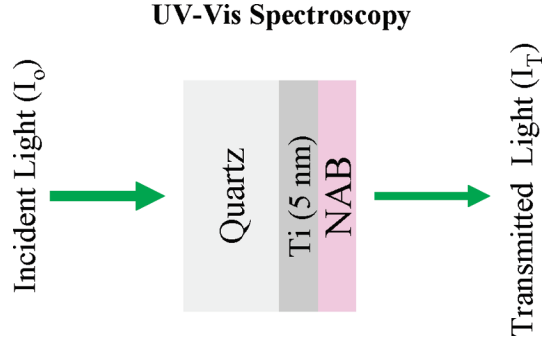

responsible for binding the molecular layer to Au surface (the characteristic IR frequencies and peaks assignments for NAB are given in Table 2). Although the peak intensities for NAB in Figure 2B (Si/SiO_x/Cr/Au(100)/Ti(5)/NAB front-side spectrum) are ~2−3x higher than that observed in Figure 2A (Si/Ti(5)/NAB/Au(100) back-side spectrum), the absolute intensities cannot be directly compared because of differences in geometry and losses in the Si. However, the fact that the relative intensities of several different bands are unaltered by Au deposition provides strong evidence that the NAB layer survives metal deposition without significant changes in structure. A detailed analysis of metal deposition effects on molecular layers will be reported separately.

In addition to Raman and IR spectroscopy, we have also used ultrathin primer metals to modify quartz substrates for use in UV/vis measurements. Figure 3A shows UV/vis absorbance spectra for quartz (Q), Q/Ti(5), Q/TiO_2(5), and Q/Ti(5)/NAB, all obtained in transmission geometry and referenced to air (as illustrated in Scheme 3). The TiO_2 layer was deposited directly from rutile as described previously,[56] and is provided for comparison. The spectrum for Q shows a uniform and low absorbance throughout the wavelength range, with a slight increase in absorbance below 275 nm. When the Ti primer layer is deposited onto Q, the absorbance increases markedly throughout the UV/vis range, and a broad feature is observed between 200 and 325 nm. This indicates that the metal is reflective and increases the optical density of the substrate, but nevertheless the sample still maintains significant optical transparency. For comparison, when oxidized TiO_2 is deposited (from rutile) onto Q, the absorbance remains close to that for unmodified Q above 400 nm, but a band is observed at 285 nm, consistent with the literature.[57] Oxidation of Ti metal can therefore be monitored by tracking the changes in UV−vis spectrum of Q/Ti. After oxidation of a Q/Ti sample at 100 °C in oxygen for one day, the UV−vis spectrum resembles that for Q/TiO_2 (from rutile), indicating that the thin layer of Ti metal can be oxidized to a passive layer of TiO_2 (data not shown). Oxidation of the Ti primer layer was studied in more detail using XPS, as discussed below. Finally, the Q/Ti(5)/NAB sample shows additional absorbance below 600 nm when compared to a Q/Ti(5) sample. To draw out the differences in absorbance between these two samples, a difference spectrum is plotted in Figure 3B as a subtraction of the Q/Ti(5) absorbance from that for Q/Ti(5)/NAB. As shown, a broad band is observed with a maximum at 340 nm, which has been attributed to NAB in previous studies.[58]

Comparison of λ_{max} of Q/Ti(5)/NAB from Figure 3B (340 nm) with that for NAB in hexane (λ_{max} = 330 nm)[58] and NAB adsorbed on optically transparent carbon (λ_{max} = 356)[58] indicates that a red-shift occurs when NAB is bonded to a substrate. This shift is most pronounced for carbon but is still apparent for films deposited onto quartz via a Ti primer. The band broadening and red shift of the NAB spectrum can be attributed either to an electronic interaction between the substrate and NAB molecular layer or to lateral interactions between chemisorbed NAB molecules on the surface.

To characterize the oxidation state of the Ti in the primer layer and to probe the nature of any chemical bonds between the molecule and the Ti primer, XPS was carried out on modified surfaces. A survey spectrum of Si/SiO_x/Ti is shown in Figure 4. Two prominent peaks are apparent: Ti(2p) and O(1s). The much smaller features such as Si(1s) at 102.8 eV are attributed to the SiO_x substrate, while peaks for species such as C(1s) at 284.8 eV can generally be attributed to adventitiously adsorbed contaminants. Figure 5 shows a high resolution spectrum for this sample in the Ti region, where a deconvolution analysis was carried out that revealed five observable features. The deconvoluted bands correspond to TiO_2 [Ti($2p_{1/2}$) at 464.7 eV and Ti($2p_{3/2}$) at 459.2 eV]; TiO [454.6 and 460.8 eV]; and Ti_2O_3 [457.9 eV].[37,59] Importantly, no peak corresponding to fully reduced Ti (i.e., 453.8

(56) Wu, J.; Mobley, K.; McCreery, R. L. *J. Chem. Phys.* **2007**, *126*, 024704.
(57) Li, X. Y.; Wang, D. S.; Luo, Q. Z.; An, J.; Wang, Y. H.; Cheng, G. X. *J. Chem. Technol. Biotechnol.* **2008**, *83*, 1558–1564.
(58) Tian, H.; Bergren, A. J.; McCreery, R. L. *Appl. Spectrosc.* **2007**, *61*, 1246–1253.
(59) Saied, S. O.; Sullivan, J. L.; Choudhury, T.; Pearce, C. G. *Vacuum* **1988**, *38*, 917–922.

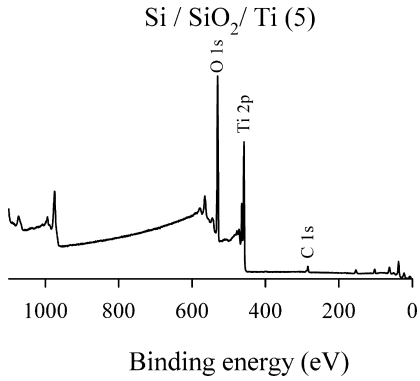

Figure 4. XPS survey spectrum of an $Si/SiO_2/Ti$ sample.

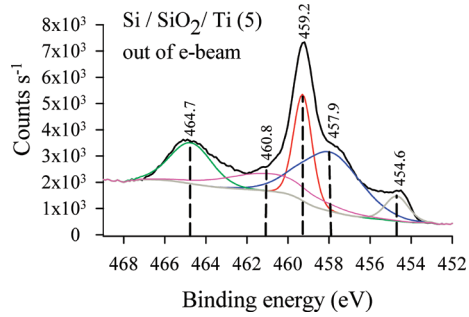

Figure 5. High-resolution XPS spectrum for $Si/SiO_2/Ti$ with several species represented as best-fit curves from a deconvolution analysis. TiO_2: $Ti(2p_{1/2})$ at 464.7 eV (green curve), $Ti(2p_{3/2})$ at 459.2 eV (red curve); TiO: 454.6 eV (gray curve) and 460.8 eV (pink curve); and Ti_2O_3 peak at 457.9 (blue curve).

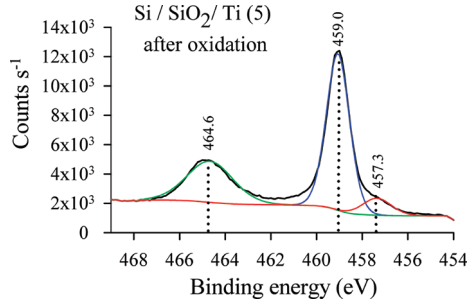

Figure 6. High-resolution XPS spectrum for $Si/SiO_2/Ti$ after exposure to a pure oxygen atmosphere for 24 h at 100 °C. Best fits: $Ti(2p_{1/2})$ at 464.6 eV (green curve), $Ti(2p_{3/2})$ at 459.0 eV (blue curve), and Ti_2O_3 peak at 457.3 eV (red curve).

eV)[50,60] is observed. This result is attributed to the high reactivity of Ti with both residual chamber gases during deposition and reaction with atmospheric oxygen upon removal of the primed substrate from the evaporation chamber. To examine the oxidation process of the Ti primer layer, several samples were treated with oxygen and heat, and the oxidation state of the layers was again evaluated using XPS.

Figure 6 shows a high-resolution XPS spectrum of $Si/SiO_2/Ti$ after exposure to pure oxygen (1 atm) for 24 h at 100 °C. Comparison of Figures 5 and 6 shows that after the treatment, most of the TiO_x is fully oxidized (i.e., occurs as TiO_2). For example, the peaks indicative of TiO_2, $Ti(2p_{1/2})$ at 464.6 eV and $Ti(2p_{3/2})$ at 459.0 eV, increase in intensity while those for less oxidized states of Ti are greatly diminished. In fact, only a small amount of Ti_2O_3 (indicated by the small peak at 457.3 eV) is indicated by the XPS data. Collectively, the results from analysis of the XPS spectra shown in Figures 4−6 shows that a Ti metal primer layer is composed of a mixture of oxides of titanium but that the film can be almost completely oxidized to TiO_2 by treatment at elevated temperatures in pure oxygen. To determine the nature of NAB bonding to the primer layer, XPS analysis was carried out on samples after deposition of the molecular layer.

Figure 7A shows an XPS survey spectrum of Si/SiOx/Ti(5)/NAB (the SiOx is thermally grown) after treating the sample in a pure O_2 atmosphere for 24 h at 100 °C (treatment carried out after NAB modification). High-resolution scans of the Ti, N, and C regions are shown in Figures 7B, 7C, and 7D, respectively. First, the analysis of the Ti region shown in Figure 7B shows that the Ti is present mainly as TiO_2, as indicated by the peaks for $Ti(2p_{1/2})$ at 464.5 eV and $Ti(2p_{3/2})$ at 458.8 eV. Small peaks at 457.1 and 455.2 eV are attributable to residual Ti_2O_3 and TiO, respectively.[61] Moreover, no distinct peak for Ti bonded directly to carbon at 454.6 eV[62] was observed after careful analysis of the high resolution spectra. Second, strong N(1s) peaks are observed in Figure 7C centered at 400.1 eV (corresponding to the azo group of the NAB molecule), and 405.9 eV (representing the nitro group of NAB). The integrated peak areas for the azo and nitro peaks are 67.25 and 32.75, respectively, which closely corresponds to the 2/1 ratio expected for the NAB molecule. Third, the C(1s) peak in Figure 7D was deconvoluted by curve fitting (as shown in the figure) into two distinct peaks: one centered at 284.7 eV that corresponds to C(1s) of sp^2 hybridized carbon in the aromatic rings of the NAB molecule,[26,63] and the other at 285.6 eV, which represents a phenyl carbon atom attached to either nitrogen or oxygen atoms.[64] No evidence of a C−Ti bond at 281.5 eV[63,65] was found. Although diazonium salt modification of Ti nanoparticles in solution reportedly results in formation of a Ti−C bond,[66] high resolution XPS analysis of Figure 7B and 7D did not provide any evidence for a Ti−C bond in the present case. Given the exposure of the Ti primer layer to the atmosphere before reaction with the diazonium reagent, the most likely surface bond is Ti−O−C rather than Ti−C.

Various experimental conditions were tested to assess their impact on the amount of modifier obtained at the surface of the substrate. To this end, the intensity of the Raman signal was followed as several variables were altered, including the thickness of the Ti, the concentration of the NAB diazonium salt in solution, and the immersion time of the primed substrate. In general, the Raman signal increased monotonically with Ti thickness, NAB

(60) Lebugle, A.; Axelsson, U.; Nyholm, R.; Martensson, N. *Phys. Scr.* **1981**, *23*, 825–827.
(61) Gonzalezelipe, A. R.; Munuera, G.; Espinos, J. P.; Sanz, J. M. *Surf. Sci.* **1989**, *220*, 368–380.
(62) Wagner, C. D.; Gale, L. H.; Raymond, R. H. *Anal. Chem.* **1979**, *51*, 466–482.
(63) Macinnes, A. N.; Barron, A. R.; Li, J. J.; Gilbert, T. R. *Polyhedron* **1994**, *13*, 1315–1327.
(64) Jordan, J. L.; Sanda, P. N.; Morar, J. F.; Kovac, C. A.; Himpsel, F. J.; Pollak, R. A. *J. Vac. Sci. Technol., A* **1986**, *4*, 1046–1048.
(65) Ihara, H.; Kumashir, Y.; Itoh, A.; Maeda, K. *Jpn. J. Appl. Phys.* **1973**, *12*, 1462–1463.
(66) Ghosh, D.; Pradhan, S.; Chen, W.; Chen, S. W. *Chem. Mater.* **2008**, *20*, 1248–1250.

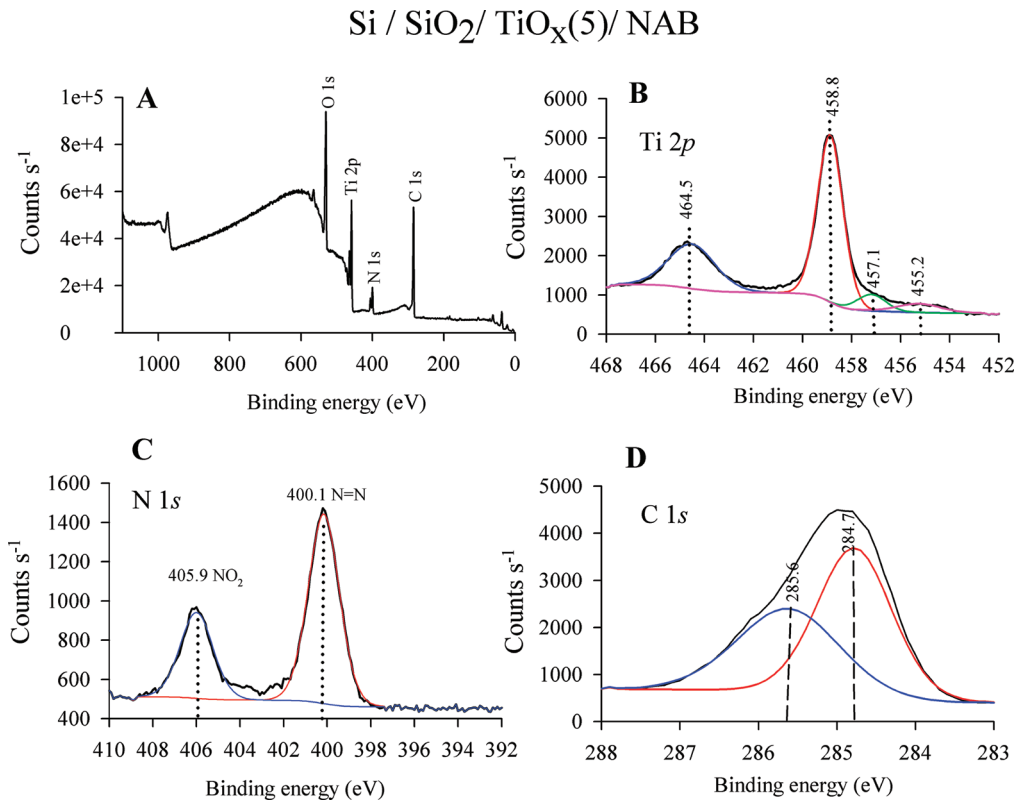

Figure 7. (A) Survey spectrum of a thermally oxidized Si wafer with a molecular layer of NAB deposited using a 5 nm Ti primer layer. (B) High-resolution spectrum in the Ti region showing peaks that correspond to Ti($2p_{1/2}$) at 464.5 eV (blue curve), Ti($2p_{3/2}$) at 458.8 eV (red curve), Ti_2O_3 at 457.1 eV (green curve), and TiO at 455.2 eV (pink curve). (C) High-resolution spectrum in the nitrogen region showing an azo N(1s) peak at 400.1 eV (red curve) and a nitro N(1s) peak at 405.9 eV (blue curve). (D) High-resolution spectrum in the carbon region showing peaks that represent C(1s) bonded to either O or N at 285.6 eV (blue curve) and C(1s) in a phenyl group at 284.7 eV (red curve).

concentration, and immersion time (see Supporting Information, Figures S-7 to S-9). For a 5 nm Ti thickness and 30 min immersion time (1 mM NAB DS), the NAB film thickness was estimated (using AFM scratching) to be 5.8 nm, indicating the formation of multilayers. Thus, the increase in the Raman signal as a function of Ti thickness, NAB concentration, and immersion time can tentatively be attributed to increases in the total amount of NAB on the substrate surface. Thus, the deposition conditions (and Ti thickness) should be optimized to achieve the desired thickness for a given application.

The stability of molecular layers deposited using a metal primer was tested by subjecting modified samples to different treatments and tracking any changes in the Raman spectral intensity. Samples of either Si/SiO_x/Ti(5)/NAB or Glass/Ti(5)/NAB were sonicated in various solvents, boiled in water, immersed into dilute acid or base, and heated. The experimental results are summarized in Table 3 and spectra are provided in the Supporting Information, Figures S-10 to S-16. As shown in the table, the peak height for the Raman band at 1600 cm^{-1} (C=C stretch) decreased in all cases, but for many conditions the loss of intensity was small. For example, sonication in acetone or immersion in weak acids or base resulted in a decrease of less than 10%. A slightly larger decrease (12%) occurs after heating the sample at 200 °C in a low vacuum, and moderate decreases are noted for sonication in ACN for 30 min or immersion in boiling water for 60 min. The results in Table 3 indicate that the molecular layer adsorbed onto the substrate through the Ti metal primer can withstand moderately concentrated alkaline and acidic solutions. Moreover, the layers show good heat resistance, consistent with a similar study in which diazonium-derived layers bound by covalent C−C bonds formed by modification of carbon surfaces using the spontaneous reduction of aryl diazonium salts were thermally stable up to 200 °C.[67] However, for the present case, a larger reduction in intensity was observed, indicating that the Ti−O−C bond appears to be slightly less thermally stable than the C−C covalent bond.

Table 3. Summary of Raman Intensity Changes for NAB after Different Treatments[a]

	before treatment	after treatment	% change
sonication in acetone	32.6 (cts s^{-1})	30.2 (cts s^{-1})	−7.3%
sonication in ACN	89.4 (cts s^{-1})	61.9 (cts s^{-1})	−30.7%
boiling water	119.8 (cts s^{-1})	91.4 (cts s^{-1})	−23.7%
0.1 M NaOH	87.7 (cts s^{-1})	83 (cts s^{-1})	−5.3%
0.1 M HCl	93.6 (cts s^{-1})	90.1 (cts s^{-1})	−3.7%
0.1 M H_2SO_4	85.6 (cts s^{-1})	81.1 (cts s^{-1})	−5.2%
heating at 200 °C	192.8 (cts s^{-1})	169.7 (cts s^{-1})	−12%

[a] The intensity of the band at ~1600 cm^{-1} (C=C ring stretch) was used as a diagnostic.

As noted earlier, Raman spectroscopy has been reported previously for characterization of molecular layers at buried interfaces and in molecular electronic junctions by using thin, partially transparent top metal contacts.[8,9,37,68] To increase the

(67) Toupin, M.; Belanger, D. *J. Phys. Chem. C* **2007**, *111*, 5394–5401.
(68) Hoagland, J. J.; Dowdy, J.; Hipps, K. W. *J. Phys. Chem.* **1991**, *95*, 2246–2250.

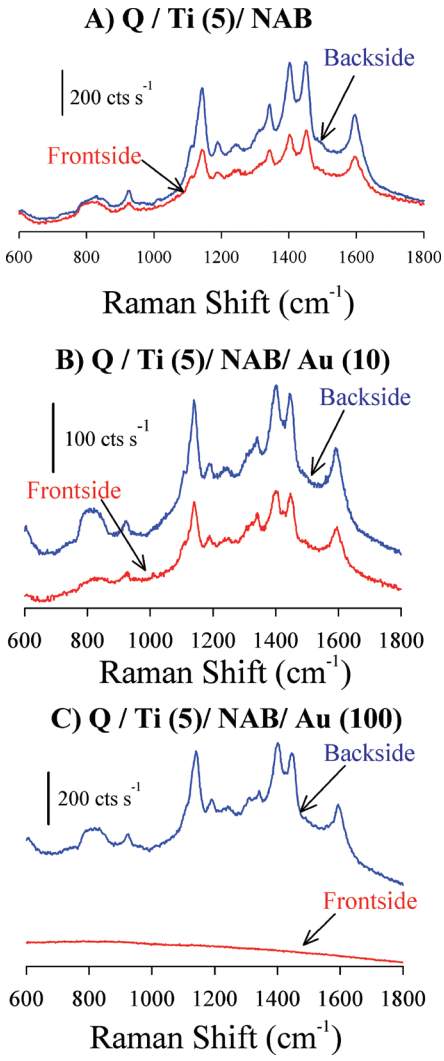

Figure 8. (A) Raman Spectra of Q/Ti(5)/NAB collected from top-side (red curve), and quartz or "backside" (blue curve). (B) Raman spectra of Q/Ti (5)/NAB after deposition of 10 nm Au metal directly on top of the molecular layer, collected from top-side (red curve), and quartz or "backside" (blue curve). (C) Raman spectra of Q/Ti (5)/NAB after deposition of 100 nm Au metal, collected from top-side (red curve), and backside (blue curve).

versatility of these experiments, we have applied Ti primer-derived adlayers to study the effect of depositing top contact materials on the structural integrity of the molecular layer. Figure 8A shows Raman spectra of Q/Ti(5)/NAB obtained from both the front-side (red curve) and from the back-side (through the primed quartz substrate, blue curve). Figure 8B shows Raman spectra of Q/Ti(5)/NAB after deposition of a thin (10 nm) transparent top metal (Au) obtained from both the front-side (through the 10 nm Au, red curve) and the back-side (through the primed quartz substrate, blue curve). As shown, the molecular signature for NAB (see Figure 1 and Table 1) is apparent in both cases, indicating that the molecular layer is not seriously damaged by metal deposition. In Figure 8B, the Raman peak intensity for NAB (and the quartz feature at 807 cm^{-1}) obtained in front-side mode is less than that observed in back-side mode because of the attenuation of the incident and scattered light by the Au layer in frontside mode. Thus, it is apparent there is a sensitivity

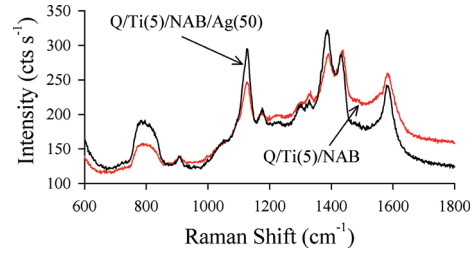

Figure 9. Raman spectrum of Q/Ti (5)/NAB obtained from the backside before (red curve) and after (black curve) deposition of 50 nm Ag.

advantage in collecting the spectrum through the "backside" (i.e., the quartz layer), of ~ 40%.

Recall that in Figure 2, the IRRAS spectrum obtained from the backside of a Si/Ti(5)/NAB/Au(100) substrate also showed that the NAB layer can easily be detected, supporting the results that Au deposition does not destroy the molecular layer. A further demonstration of the utility of back-side Raman is demonstrated in Figure 8C, where both front- and back-side Raman spectra are shown for a Q/Ti(5)/NAB sample with 100 nm of Au deposited directly onto the molecular layer (as illustrated in Scheme 1). The backside spectrum obtained through the Q substrate (blue curve) is similar to that observed for only 10 nm of Au (Figure 8B, blue curve), in both structure and intensity. However, the front-side spectrum obtained (Figure 8C, red curve) shows that no molecular signature for the molecular layer can be obtained. Since the backside spectrum (blue curve) shows a clear Raman spectrum for NAB, the "disappearance" of the spectrum in front-side mode (for the exact same sample) must be due to minimal transmission through the 100 nm thick Au layer. Thus, molecular layers buried under relatively thick top contact materials and with minimal optical transparencies can be characterized using the back-side method if an appropriate substrate support is used (e.g., quartz for Raman or Si for IR).

To test the generality of these observations, a different top contact material was chosen. Figure 9 compares the backside spectra of Q/Ti(5)/NAB before and after deposition of 50 nm of Ag. Metals such as Ag, Cu, and Ti can reduce NAB, as evidenced by a reduction in the ratio of the peak intensity at 1406 cm^{-1} to that at 1451 cm^{-1} (N=N stretches).[3,9] Indeed, in Figure 9, the ratio decreases from 1.1 to 0.99 after Ag deposition. A detailed analysis of metal deposition effects on molecular layers will be reported separately.

CONCLUSIONS

This work has shown that ultrathin layers of reactive metals can be used as a primer to prepare a variety of substrate materials for modification via the reduction of aryl diazonium ions. The molecular layers on the surface of the Ti primer are stable to sonication, aqueous acids and bases, and moderate heating. Diazonium reagents can be made from a wide variety of aromatic amines, and the Ti primer was shown to enable bonding of diazonium-derived radicals to glass, quartz, Au, Al, and polyethylene. Since Ti is quite reactive and bonds to both conducting and insulating surfaces, its use as a primer should be applicable to a wide variety of materials. Modification of transparent substrates enables UV−vis, FTIR, and Raman spectroscopy for characterization of the molecular layer at buried interfaces after

deposition of a top contact regardless of its thickness. An NAB molecular layer bonded to quartz through a Ti primer layer shows minimal changes to its Raman spectrum following deposition of up to 100 nm of Au by direct electron-beam deposition.

ACKNOWLEDGMENT

This work was supported by NSERC, the National Institute for Nanotechnology, and the University of Alberta. The National Institute for Nanotechnology is operated as a partnership between the National Research Council and the University of Alberta and is jointly funded by the Government of Canada, the Government of Alberta, and the University of Alberta. Portions of this work were carried out at the University of Alberta NanoFab facility. We also thank Dimitre Karpuzov at the University of Alberta ACSES facility for obtaining XPS spectra. Amr M. Mahmoud acknowledges the Analytical Chemistry Department, Faculty of Pharmacy at Cairo University, Egypt, for granting a leave of absence.

SUPPORTING INFORMATION AVAILABLE

Additional information as noted in the text. This material is available free of charge via the Internet at http://pubs.acs.org.

Received for review May 14, 2009. Accepted July 2, 2009.

AC901052V